BJRS

BRAZILIAN JOURNAL
OF
RADIATION SCIENCES
11-01A (2023) | 01-17 | e2118

Monte Carlo simulation-aided design of a thermal neutron generator system from ^{241}Am-Be isotopic sources

Orozco[a,c], A. C.; Federico[b,c], C. A.; Gonçalez[b,c], O. L.

[a] *Instituto de Aeronáutica e Espaço/Serviço de Proteção Radiológica, CEP 12.228-904, São José dos Campos, SP – Brasil*

[b] *Instituto de Estudos Avançados/Divisão de Energia Nuclear, CEP 12.228-001, São José dos Campos, SP – Brasil*

[c] *Instituto Tecnológico de Aeronáutica/Programa de Pós-graduação em Ciências e Tecnologias Espaciais, CEP 12.228-900, São José dos Campos, SP – Brasil*

odairlelisgoncalez@gmail.com

ABSTRACT

Collimated thermal neutron beams are obtained from neutron extraction channels in nuclear reactors for various applications in research and technology, such as neutron imaging techniques (neutron radiography, neutron radioscopy, neutron tomography, and neutron-based autoradiography). Practical setups for neutron radiography using ion beams from particle accelerators and radioisotopic sources of fast neutrons have been also developed. However, only radioisotopic sources enable autonomous and transportable thermalization systems that can produce thermal neutron collimated beams. This work presents the performance results for a prototype of a compact system that generates a collimated beam of thermal neutrons using low-activity isotopic ^{241}Am-Be sources. It was designed with the aid of Monte Carlo simulation using the PHITS v 3.17 program. Experimental measurements of the fluence of the neutron beam produced by the built prototype showed good agreement with the simulated values by the Monte Carlo method.

Keywords: **neutrongraphy, thermal neutrons, Monte Carlo, simulation, PHITS.**

ISSN: 2319-0612
DOI: https://doi.org/10.15392/2319-0612.2023.2118
Submitted: 2022-09-30
Accepted: 2023-07-11

1. INTRODUCTION

Collimated thermal neutrons beams are obtained from neutron extraction channels in nuclear reactors for several applications in research and technology, such as neutron imaging techniques (neutron radiography, neutron radioscopy, neutron tomography, and neutron-based autoradiography) and materials analysis (prompt gamma-ray activation analysis, neutron diffraction, neutron scattering, neutron polarization, neutron reflectometry, neutron interferometry, etc.) [1 – 4].

Neutron imaging – neutron radiography or neutrongraphy – has been used in a wide variety of industrial research and non-destructive testing (NDT) applications since early 1960 [4-6]. Its use, however, requires that the experimental arrangement is located near the nuclear reactor core and that the objects to be irradiated are brought to this location.

Practical setups for neutrongraphy using ion beams from particle accelerators and radio isotopic sources of fast neutrons have been also developed [7-8]. However, only radio isotopic sources enable autonomous and transportable thermalization systems that produce thermal neutron collimated beams.

Long-time thermal neutron systems based on sealed fast neutron sources, such as ^{241}Am-Be or ^{252}Cf, embedded in large (few cubic meters) polyethylene or graphite moderator assemblies, have been traditionally used for neutron dosimetry at several facilities, like NBS (USA) [9], Polytechnic of Salt Bank (England) [10], IRSN (France) [11, 12], ENEA Radiation Protection Institute (Italy) [13, 14, 15], PTB (Germany) [16], CERN [17], Arizona State University (USA) [18], JAEA-FRS (Japan) [19], KRISS (Korea) [20] and others. In these facilities, a quasi-isotropic thermal neutron flux inside a cavity is used to irradiate detectors, dosimeters, and, in some ones, large devices as well as phantoms [15]. But none of them could be used as a thermal neutron Howitzer that provides a beam of thermal neutrons similar to what would be emitted by a point source, such as the required for neutrongraphy. On the other hand, in Brazil, at the Neutron Metrology Laboratory of the Institute of Radioprotection and Dosimetry (IRD) there is such a system, whose ^{241}Am-Be sources were calibrated and referenced to a national standard [21].

The current engineering challenge for neutrongraphy is to produce a proper thermal neutron beam to obtain the radiographic image with neutrons employing systems with isotopic sources of fast

neutrons enabling to use neutrongraphy technique routinely outside the sites of particles accelerator or the nuclear reactor. This work aims to added a contribution to this task.

The purpose of the work reported in this paper was to build a thermal neutron howitzer prototype that produces a thermal neutron beam meeting the requirements of their application in neutrongraphy.

The performance results of such a system that generates a collimated beam of thermal neutrons using low-activity isotopic sources of ^{241}Am-Be are reported in this paper. The system was designed with the aid of Monte Carlo simulation using the PHITS program [22] to determine the geometry and the construction materials that would maximize the fluence of thermal neutrons in the extracted beam and, also, that minimize the contamination of the beam with epithermal and fast neutrons and with X- and gamma-radiation. The design optimization procedure with the aid of Monte Carlo simulations was presented in previous work [23].

In this work, the results of experimental measurements of the extracted thermal neutron beam of the howitzer are compared to those in the project beam performance simulation as built.

2. MATERIALS AND METHODS

The system was designed and its performance was optimized with the aid of Monte Carlo simulation using the updated PHITS v 3.17 program [22], from an old rectangular geometry howitzer existing in the Laboratory of Ionizing Radiation of the Institute of Advanced Studies (São José dos Campos, Brazil) [23]. In the final design, the system has a cylindrical geometry. Figure 1 shows the design as built from PHITS' graphical utility.

All simulations were performed with 10^8 to 10^9 source particles, in the form of 200 to 2,000 batches with 500,000 source particles per batch, respectively, with multiprocessing in a Workstation of 20 CPU XEON 2.7 of the IEAv's Aerospace Dosimetry Laboratory so that statistical error was less than 1% in all cells of interest. The processing time ranged from 8 to 48 hours and was not necessary to apply variance reduction techniques.

Measurements of the thermal neutron fluence of the beam emitted by the system were performed to compare the simulation with the experimental results. The thermal neutron beam produced was calibrated by the transfer instrument method. In this method, the detector used in neutron fluence

measurements was calibrated in a thermal neutron reference beam at the Neutron Metrology Laboratory of the Institute of Radioprotection and Dosimetry of the National Nuclear Energy Commission (LN/IRD/CNEN) [21].

Figure 1: *System (howitzer) schematic drawings*

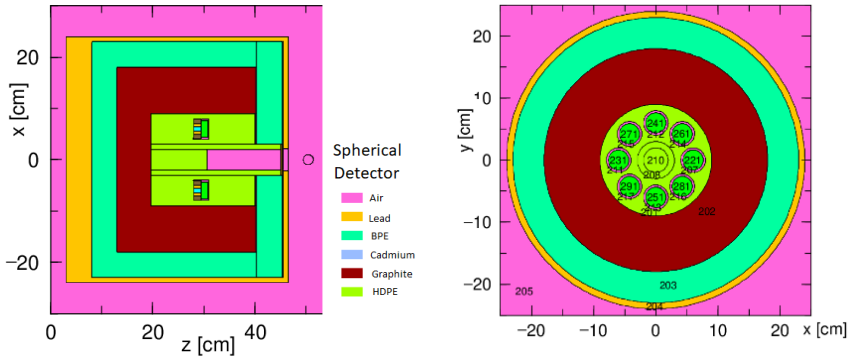

(a) Longitudinal cut (b) transversal section

Briefly, the thermal neutron collimated beam generating system (howitzer) consists of a central core of high-density polyethylene (0.949 g/cm^3) of cylindrical shape (18 cm in diameter and 20 cm in height). This core has a beam extraction central channel of 4 cm in diameter and, around its central axis, eight sources of ^{241}Am-Be, with an activity of 100 mCi each, are distributed in symmetrically opposite positions at 6 cm from its central axis. The sources accommodation cavities are 10 cm from the frontal face of the polyethylene cylindrical block. After the insertion of sources, the remaining spaces are filled with polyethylene plugs. The main purpose of polyethylene is to moderate the fast neutrons produced by the sources. This thermalizing core is housed inside a hollow graphite cylinder, with a wall thickness of 8.5 cm, which serves as a neutron reflector and moderator.

This assembly is shielded by a cover (5 cm) of borated polyethylene (10% of B, in weight) and an additional outer layer of lead (1.2 cm) to reduce the leakage of neutrons and gamma radiation to the environment. Two cadmium sheets, 5.4 cm apart, each one with a 4 cm diameter central hole, are placed on the front side of the system to produce the beam collimation and to reduce unwanted leakage of non-collimated thermal neutrons in the beam direction. The first cadmium sheet is positioned at the top of the central polyethylene cylinder and the second is placed after the borated polyethylene shield, with the center of the respective holes overlapping the central axis of the thermal

beam extraction channel. A 3 mm thick lead filter is placed at the exit of the extraction channel to reduce contamination of the beam with X-rays and gamma rays.

The system is completely dismountable and the parts matching allow the fast loading of neutron sources. Eight 100 mCi sealed neutron sources of ^{241}Am-Be were used, reaching a total activity of 0.8 Ci of ^{241}Am isotope with a total neutron emission rate of 1.968×10^6 n/s. The neutron sources were calibrated with a Long Counter used as a calibration transference instrument. The overall uncertainty of the neutron sources emission is about 2.45%. The assembling of the system is shown in Figure 2. The sketch of ^{241}Am-Be neutron sources is shown in Figure 3 and the properties of the materials that constitute them are given in Table 1. In simulations, 8 cylindrical volumetric sources of neutrons with isotropic emission and the multigroup ISO 8529 [24] energy spectrum of ^{241}Am-Be from 10 keV to 10.5 MeV for source-term were used.

Figure 2: *Pictures of the system assembling*

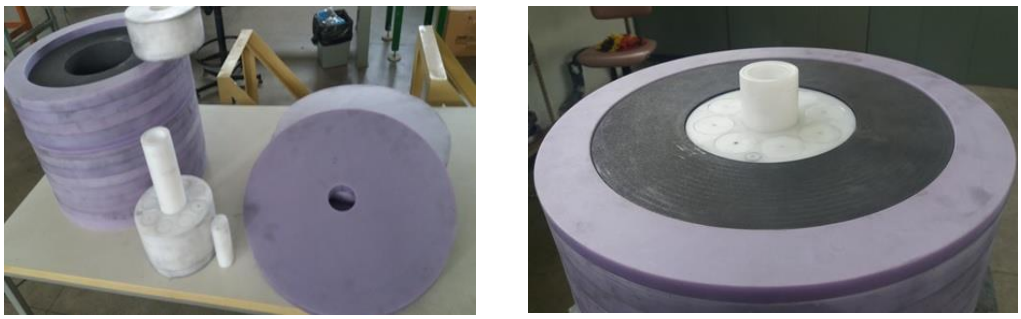

Figure 3: *^{241}Am-Be neutron source sketch (dimensions in mm)*

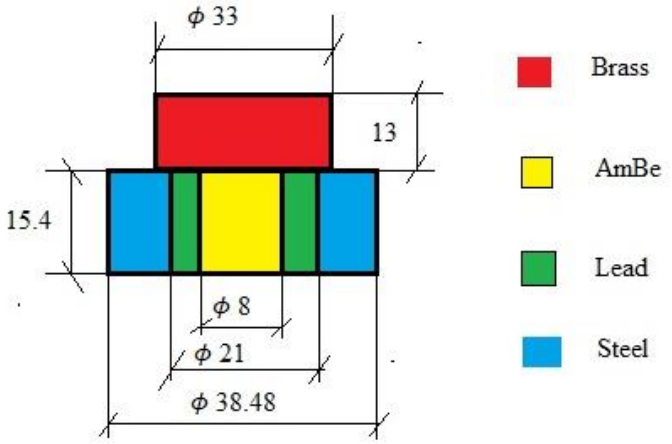

Table 1 – Neutron sources material composition

Material	Mass Composition	Density (g/cm^3)
Brass	Cu 66.5%; Zn 32.6%; Sn 0.3%; Pb 0.5%; Fe 0.1%	8.07
Am-Be	Am 20%; O 60%; Be 20%	7.34
Lead	Pb 100%	11.3
Steel	Fe 99.5%; C 0.5%	7.87

PHITS simulations were run in order to assess the fluences normalized per neutron emitted by the sources. In this arrangement, the absolute values of neutron fluences are calculated by multiplying the simulation results by the neutron emission rate from the sources. Therefore, the results presented in this work are valid for neutron sources with lower or higher activities that could be used in this arrangement. In that case, it would be necessary to adjust the thickness of the shielding for radiological protection purposes (borated polyethylene and lead).

The thermal neutron detector used was a ^{3}He proportional counter tube of 2.54 cm in diameter and 15.24 cm in length from Reuter-Stokes (USA) model RS-P4-0806-271. The detector tube was completely surrounded by a 0.5 cm thick cadmium cover with a 1 cm diameter hole in its central part (See Figure 4), which serves as an entry window for thermal neutrons. The detector was connected to a Standard EG&G Ortec NIM conventional pulse counting arrangement (Figure 4).

Figure 4: *Thermal neutron detector set-up: (a) ^{3}He detector and cadmium cover, (b) Scheme of the counting system and (c) Picture of MCA pulse amplitude spectrum for neutron pulses selection*

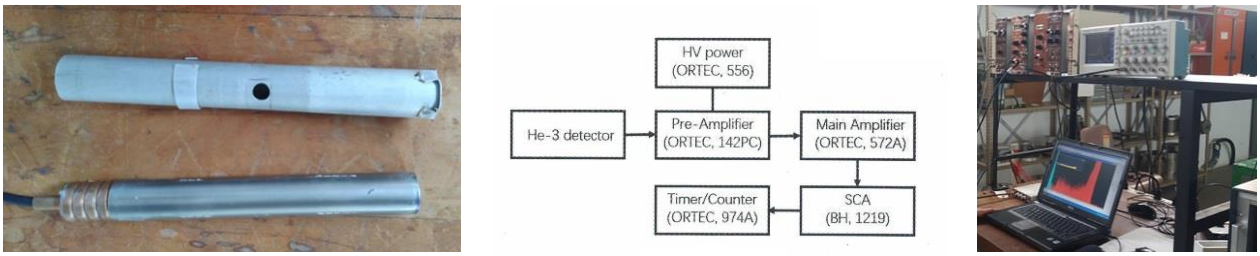

(a) (b) (c)

The technique for selecting the counts due only to thermal neutrons consists of applying a cadmium shutter over the thermal neutron entrance window and considering the difference between the counts of the detector exposed to the neutron beam with the shutter open and the one with the

shutter closed. This setup emulates a small-size thermal neutron detector for directional fluence with a 1 cm diameter circular entrance window.

For the PHITS simulations, the following primary radiation sources were considered:

a) Neutrons: Multigroup energy spectrum from 10 keV to 10.5 MeV [24]

b) Gamma rays emitted by the ^{241}Am-Be source

The gamma rays emitted by the ^{241}Am-Be source are:

a) ^{241}Am alpha decay gamma lines: 26.34 keV (2.27%) and 59.54 keV (35.64%) [25, 26]

b) Prompt gammas emitted in the ^{9}Be(α,n)^{12}C reaction that takes the residual carbon nucleus to the first excited state of 4,438 keV, where the gamma/neutron ratio is 0.575 [27]

Therefore, it was decided to carry out two separate simulations for the gamma radiation emitted by the ^{241}Am-Be source. The first one was for 26.34 and 59.54 keV lines, with relative intensities of 0.05988 and 0.94012 (note that the sum must be equal to 1). The fluences and doses simulated for this source should be multiplied by the activity of the source and the total intensity of the gamma lines (37.91% of each alpha decay). The second simulation was for the 4438 keV line with 100% probability. The score of this second simulation is linked to the neutron emission in the ^{9}Be(α,n)^{12}C reaction and, therefore, must be multiplied by the factor 0.575 gamma/neutron produced and by the neutron emission rate of the ^{241}Am-Be sources.

The transport of gamma emitted by the interactions of neutrons with the materials of the system was done together with the simulation of the transport of neutrons, as these gamma rays are directly associated with the reactions of neutrons with these materials.

An important function included PHITS is the event generator mode for low-energy neutron interaction, that is a new treatment of radiation behavior for the transport of the low energy neutrons, in which are combined the nuclear data and a special reaction model so as to trace all higher correlations among ejectiles, keeping the energy and momentum conservation in a collision [27, 28]. The scattering matrix S(α, β) treatment is already included in the treatment of low energy neutron transport in PHITS version 3.17 by default. In section 5.2.18 of the PHITS manual (“Physical parameters for low energy neutrons”) we only have the options of using S(α, β) with or without interpolation. In this work simulations we use the default value of the “isaba” parameter (isaba = 0), which means using the matrix S(α, β) without interpolation, which is more suitable for bulky targets.

3. RESULTS AND DISCUSSION

Table 2 presents the results of the determination of the calibration factor of the thermal neutron detector used in this work in the standard reference field of LN/IRD/CNEN [21]. The distances in Table 2 are referenced to the beam exit hole at the front face of the IRD's thermal neutron system and its effective center is located 19.76 cm inside with 0.10 cm standard deviation. The standard deviation of distances from the effective center to the detector measurement positions is mainly due to the effective center standard deviation and we take over equal to 0.10 cm. The beam intensity obeys the inverse square law of the distance to the effective center. The average calibration factor obtained is 2.281 $n.cm^{-2}$ per count with 0.028 $n.cm^{-2}$ per count standard deviation. This average calibration factor and its standard deviation were calculated by the average of calibration factors of each detector position weighted by the inverse square of its respective standard deviation.

Table 2: Thermal neutron detector calibration data in the LN/IRD/CNEN reference field

Distance to beam hole (cm)	Reference fluence rate ($n.cm^{-2}.s^{-1}$)	Detector count rate ($count.s^{-1}$)	Calibration factor ($n.cm^{-2}.count^{-1}$)
50.1 ± 0.10	596.03 ± 5.96	261.82 ± 1.07	2.276 ± 0.025
60.4 ± 0.10	452.70 ± 4.53	201.22 ± 1.05	2.250 ± 0.025
69.7 ± 0.10	363.47 ± 3.63	161.44 ± 0.66	2.251 ± 0.024
80.3 ± 0.10	290.54 ± 2.91	127.17 ± 0.71	2.285 ± 0.026
100.3 ± 0.10	201.81 ± 2.02	88.08 ± 0.38	2.291 ± 0.025
120.2 ± 0.10	148.50 ± 1.49	63.72 ± 0.83	2.331 ± 0.038
149.5 ± 0.10	101.54 ± 1.02	44.97 ± 0.71	2.258 ± 0.042
200.2 ± 0.10	60.13 ± 0.60	26.15 ± 0.54	2.299 ± 0.053

Table 3 presents the results of 10^8 stories of PHITS simulation and experimental measurements of the neutron beam extracted from the system at distances from 4.9 to 39.9 cm. The thermal fluence refers to the spectrum region from 10^{-3} to 0.55 eV. The distances in Table 3 are referenced to the beam exit hole located at the front face of the system. The beam intensity obeys the law of the inverse square of the distances of the measurement positions to the effective center. Because the distances were taken with a high-precision digital laser tape, the standard deviation of distance from the

effective center to the detector measurement positions taken are mainly due to the effective center standard deviation and we take over equal to 0.015 cm as explained in the following paragraph.

The effective center is located inside the beam extraction channel 4.683 cm from the exit hole with 0.015 cm standard deviation. This position of effective center was obtained by standard least square fit of the simulation results to the law of the inverse square of the distances.

Figure 5 shows the variation of measured thermal neutron fluence rate at the beam centerline with distance from effective center, where the independent variable x = 1/(square of distance) was used in the graph for visualization on a linear scale.

Figure 5: *Measured thermal neutron fluence rate*

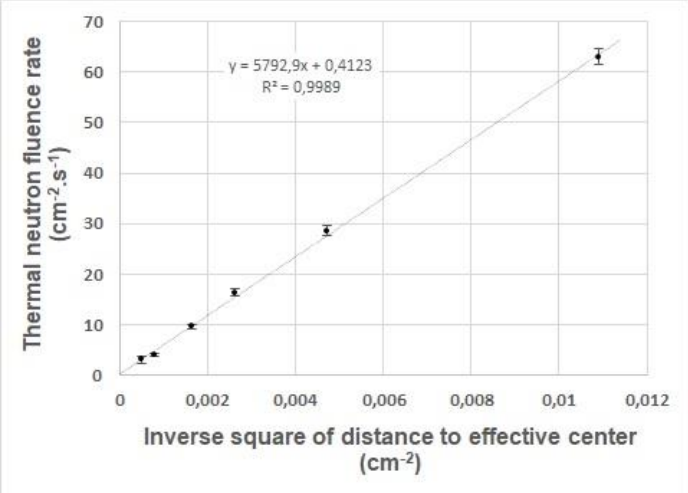

Considering that both simulated fluence and experimental measured fluence come from a large number of event counts, we can take these to be Gaussian distributed measurements, where we have values of the sample mean (μ_1 and μ_2) and respective standard deviation of mean ($\sigma_{\mu 1}$ and $\sigma_{\mu 2}$). The difference between μ_1 and μ_2 will also follow a Gaussian distribution, with standard deviation of the mean equal to the square root of the sum of squares of $\sigma_{\mu 1}$ and $\sigma_{\mu 2}$. Thus, we can apply the Z-test for the equality of two means for all pairs of data in Table 3, in order to assess the consistency between the simulation and the experimental measurement (i.e., the null hypothesis H_0 is that $\mu_1 = \mu_2$). In this case, for 95% confidence interval, the z-critical values will be ±1.96. As can be seen in the last column of Table 3, all z-values found are inside the z-critical interval, which show, with significance level

$\alpha = 0.05$ that H_0 cannot be refuted, i.e., there is agreement between these two methods of assessment of the thermal neutron fluence in this howitzer.

Table 3: Simulation and measurements of thermal neutron beam fluence

Distance (cm)	Thermal neutron fluence rate ($n.cm^{-2}.s^{-1}$)		Difference μ_1-μ_2	z-value $(\mu_1-\mu_2)/\sigma_{\mu 1-\mu 2}$
	μ_1 = Simulated	μ_2 = Measured		
4.90 ± 0.015	68.9 ± 3.4	63.0 ±1.5	5.90 ± 3.72	1.587
9.90 ± 0.015	28.4 ± 1.4	28.59 ± 0.94	-0.19 ± 1.69	-0.113
14.90 ± 0.015	15.78 ± 0.79	16.36 ± 0.68	-0,58 ± 1.04	-0.556
19.90 ± 0.015	10.06 ± 0.50	9.74 ± 0.46	0.32 ± 0.68	0.471
30.90 ± 0.015	4.87 ± 0.24	4.10 ± 0.32	0.77 ± 0,40	1.925
39.90 ± 0.015	3.15 ± 0.16	3.190 ± 0.067	-0.040 ± 0.173	-0.231

A visual way of the Z-test is through the Bland-Altman-plot, that is used to analyze the agreement of different assays or methods of analysis [30]. This plot shows the values of the difference between the corresponding measurement pairs (μ_1 - μ_2) as a function of the arithmetic mean between the respective measurement values: $(\mu_1 + \mu_2)/2$. Figure 6 shows the Bland-Altman-plot for the data in Table 3, where the differences between the measurements were normalized by the respective mean values, to facilitate visualization. The continuous horizontal line represents the arithmetic mean of the differences (μ_1 - μ_2) and the dotted lines shows the values that correspond to the 95% confidence interval (mean ± 1.96 × Standard deviation of μ_1 - μ_2).

Figure 6: Bland-*Altman-plot for 95% confidence interval*

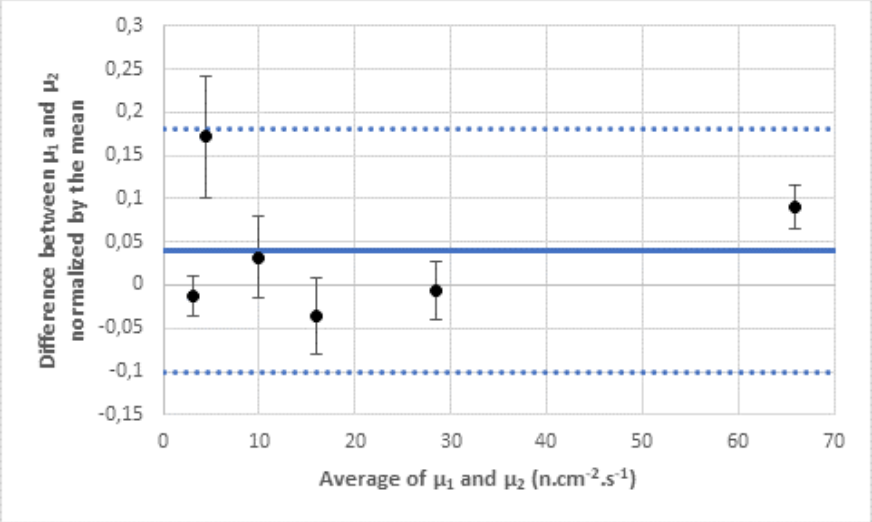

In figure 7, it is shown the intensity mapping at the beam cross section located 5 cm from the beam hole exit obtained with the thermal neutron detector and, also, by PHITS simulation with 10^8 stories. It can be noticed that the intensity of the beam is homogeneous in a circular portion with a diameter of 2 cm around the center of the beam line. Nevertheless, it decreases to approximately 90% of the maximum value at a diameter of 4 cm.

Figure 7: *Intensity mapping in the beam cross section 5 cm from the beam hole exit*

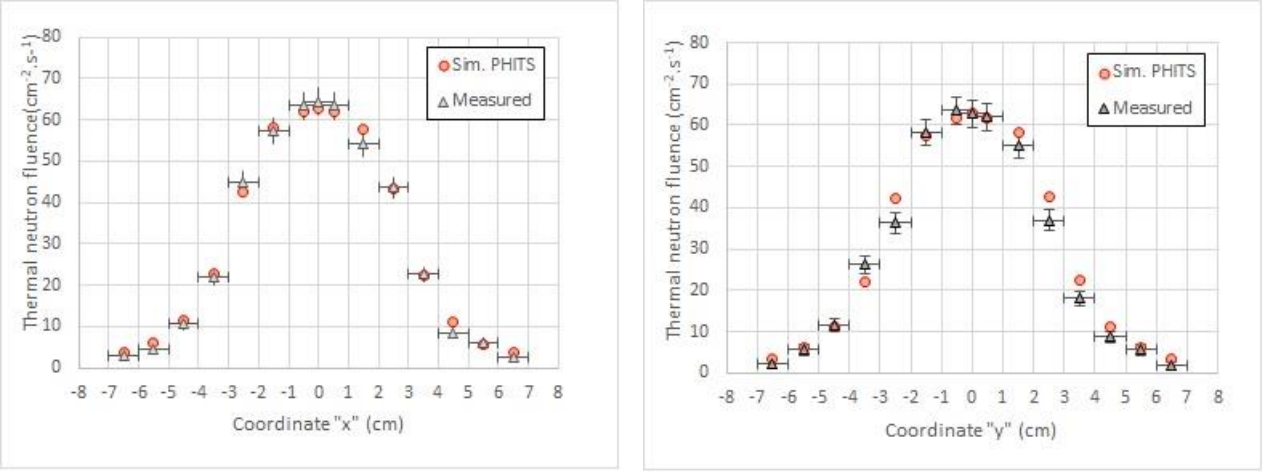

These results indicate that a significant development of the beam collimation system will be necessary to meet the requirements of neutron radiography imaging resolution [28, 29]. The elaboration of an adequate project of this system could be greatly facilitated and speeded up with the use of the PHITS program.

For simulations of the thermal neutron beam contamination with X-rays and gamma-rays, it was used a 1 cm diameter and 1 mm thickness photon absorbed dose detector filled with air centralized with the central line of the neutron beam at a distance of 1.2 cm from exit window of the neutron beam. The result of the transport simulation for gamma radiation emitted by alpha decay of ^{241}Am was added to the result of neutron transport simulation with tracking of gamma- and X-rays produced by ^{9}Be(alpha, n)^{12}C reaction in ^{241}Am-Be neutron source and, also, with prompt gamma-rays from neutron reactions with all system materials nuclei. The value obtained was 1.585 ± 0.027 nGy/s due to 4.438 keV gamma rays emitted by the ^{241}Am-Be neutron sources added to 3.355 ± 0.064 nGy/s

due to all prompt gammas in thermal neutron captures. The neutron fluence rate in this point is 204.32 ± 0.31 neutron/cm^2.s, thus, the gamma contamination in the thermal neutron beam is 41.363 ± 0.085 (neutron/cm^2)/nGy.

The simulation with 10^9 particles-source showed that ^{241}Am alpha decay gamma lines of 26.34 keV and 59.54 keV from the neutron sources do not contribute with the gamma-ray dose at this beam window position.

The 2.23 MeV gamma line from thermal neutron capture in Hydrogen is the most prominent in the simulated gamma spectrum in neutron transport, with a fluence of 428.1 ± 1.2 photons.cm^{-2}.s^{-1} at 1.2 cm from the exit window of the neutron beam at centerline.

In this same position in the neutron beam, the ratio of epithermal and fast neutron fluency (0.55 eV to 10.5 MeV) to thermal neutron fluency (10^{-3} to 0.55 eV) obtained by simulation was (36.375 ± 0,061) %. This qualification parameter is lower than that exhibited by IRD's system, about 70% [21].

No gamma spectrum measurements and fast fluency of neutrons have not yet been performed to compare with these simulation results.

4. CONCLUSIONS

This system was built as a concept demonstrator of a compact thermal neutron generator to be applied in neutrongraphy, but it can be also used as a laboratory bench thermal neutron system for dosimeters and small-size neutron monitors testing, as long as it is calibrated against a certified and traced reference standard [21].

The beam extracted from the system meets the main requirements for its use in neutrongraphy, which are: emission equivalent to a point source located at its effective center and the ratio of neutron fluence rate to gamma- and x-rays dose rate in the beam is less than 10 (n/cm^2)/nGy [3]. Contamination of the thermal beam by epithermal and fast neutrons does not interfere with the image quality of neutrongraphy because the image sensor is selective for thermal neutrons generally. However, for calibration of detectors and dosimeters, it will be necessary to use the cadmium cover technique to do thermal/non-thermal discrimination.

The neutron fluences results obtained from the performed PHITS computational simulation and from the prototype measurements in the laboratory with calibrated low activity isotopic neutrons sources presented very close values, indicating that the absolute results of these simulations by the PHITS code are close realistic since was not necessary apply any normalization factor or other benchmark experiment.

As pointed out by Sato [22] the code PHITS results had been showed accurate and precise for radiation systems in various applications that require particle and photons transport, where analytical solutions are difficult or imprecise. The present work corroborates this in this regard. It was also very useful in saving time for the final project of our prototype, as the manufacture of partial development prototypes was not required.

However, our results show that it is still necessary to improve the extracted beam collimation system and increase the thermal/non-thermal ratio in the neutron beam. The results of the present work are encouraging to pursue the necessary adjustments in this system using the PHITS code as a good project support tool.

ACKNOWLEDGMENT

The authors are grateful for the support of the CITAR Project, which is funded by the national Study and Project Funding agency - FINEP.

REFERENCES

[1] INTERNATIONAL ATOMIC ENERGY AGENCY. **Use of neutron beams for low and medium flux research reactors: radiography and materials characterization**. IAEA-TECDOC-837. Vienna: IAEA, 1993.

[2] INTERNATIONAL ATOMIC ENERGY AGENCY. **Neutron imaging: A non-destructive tool for materials testing.** IAEA-TECDOC-1604. Vienna: IAEA, 2008.

[3] BERGER, H. **Neutron Radiography: Methods, capabilities, and applications**. New York: Elsevier (1965).

[4] CHANKOW, N. Neutron Radiography. **Defense Science Journal**, v. 32, n. 3, p. 259-273, 1982.

[5] STROBL, M.; MANKE, I.; KARDJILOV, N.; HILGER, A.; DAWSON, M.; BANHART; J. Advances in neutron radiography and tomography. **Journal of Physics D: Applied Phys**, v. 42 (2009) 243001.

[6] CRAFT, A. E.; HILTON, A.; PAPAIOANNOU, G. C. Characterization of a neutron beam following reconfiguration of the Neutron Radiography Reactor (NRAD) core and addition of new fuel elements. **Nuclear Engineering and Technology**, v. 48, n. 1, p. 200-210, 2016.

[7] FANTIDIS, J. G.; NICOLAOU, G. E. Development of a neutron radiography system based on a 10 MeV electron Linac. **Majlesi Journal of Electrical Engineering**, v.14, n. 4, p. 21-28, 2020.

[8] ZHAO, D.; JIA, W.; HEI, D.; CHENG, C.; LI, J.; CAI, P.; CHEN, Y. Design of a neutron shielding performance test system based on Am–Be neutron source. **Radiation Physics and Chemistry**, v. 193, April 2022, article 109954.

[9] DE JUREN J. A.; ROSENWASSER H. Absolute calibration of the NBS Standard Thermal Neutron Density. **Journal of Research of the National Bureau of Standards**, v. 52, n. 2, p. 93-96. 1954.

[10] PRACY, M.; HAQUE, A.K.M.M. Neutron howitzer design. **Nuclear Instruments and Methods**, v. 135, n. 2, p. 217-221, 1976.

[11] LACOSTE, V.; GRESSIER, V.; MULLER, H.; LEBRETON, L. Characterization of the IRSN graphite moderated Americium–Beryllium neutron field. **Radiation Protection Dosimetry**, v. 110, n. 1-4, p. 135–139, 2004.

[12] LACOSTE, V. Design of a new IRSN thermal neutron field facility using Monte-Carlo simulations. **Radiation Protection Dosimetry**, v. 126, n. 1-4, p. 58–63, 2007.

[13] GUALDRINI, G.; BEDOGNI, R.; MONTEVENTI, F. Developing a thermal neutron irradiation system for the calibration of personal dosemeters in terms of $H_P(10)$. **Radiation Protection Dosimetry**, v. 110, n. 1-4, p. 43–48, 2004.

[14] BEDOGNI, R.; SACCO, D.; GÓMEZ-ROS, J. M.; LORENZOLI, M.; GENTILE, A.; BUONOMO, B.; POLA, A.; INTROINI, M.V.; BORTOT, D.; DOMINGO, C. ETHERNES: A new design of radionuclide source-based thermal neutron facility with large homogeneity area. **Applied Radiation and Isotopes**, v. 107, p. 171-176, 2016.

[15] BEDOGNI, R.; SPERDUTI, A.; PIETROPAOLO, A.; PILLON, M.; POLA, A.; GÓMEZ-ROS, J.M. Experimental characterization of HOTNES: A new thermal neutron facility with large homogeneity area. **Nuclear Instruments and Methods in Physics Research A**, v. 843, p. 18–21, 2017.

[16] LUSZIK-BHADRA, M.; REGINATTO, M.; WERSHOFEN, H.; WIEGEL, B.; ZIMBAL, A. New PTB thermal neutron calibration facility: first results. **Radiation Protection Dosimetry**, v. 161, n. 1-4, p. 352–356, 2014.

[17] FERRULLI, F.; SILARI, M.; THOMSEN, F.; ZORLONI, G. A thermal neutron source for the CERN radiation Calibration Laboratory. **Applied Radiation and Isotopes**, v. 178, 2021, article 109977.

[18] ANDERSON, B. C.; HOLBERT, K. E.; BOWLER; H. Design, construction, and modeling of a 252Cf neutron irradiator. **Science and Technology of Nuclear Installations**, v. 2016, article 9012747.

[19] NISHINO, S.; TANIMURA, Y.; EBATA, Y.; YOSHIZAWA, M. Development of the graphite-moderated neutron calibration fields using 241Am-Be sources in JAEA-FRS. **Journal of Radiation Protection and Research**, v. 41, n. 3, p. 211-215, 2016.

[20] KANG, S.; KIM, J.; KIM, J.H.; PARK, H.; PARK, H.; YOON, Y. S. Neutron irradiation facilities, neutron measurement system, and mono-energetic neutron fields at KRISS. **Journal of the Korean Physical Society**, v. 82, p. 586–594, 2023.

[21] ASTUTO, A.; SALGADO, A. P.; LEITE, S. P.; PATRÃO, K. C.; FONSECA, E. S.; PEREIRA, W. W.; LOPES, R. T. Thermal neutron calibration channel at LNMRI/IRD. **Radiation Protection Dosimetry**, v. 161, n. 1-4, p. 185-189, 2014.

[22] SATO, T.; IWAMOTO, Y.; HASHIMOTO, S.; OGAWA, T.; FURUTA, T.; ABE, S.; KAI, T.; TSAI, P.; MATSUDA, N.; IWASE, H.; SHIGYO, N.; SIHVER, L.; NIITA, K. Features of

Particle and Heavy Ion Transport Code System (PHITS) version 3.02. **Journal of Nuclear Science and Technology**, v. 55, n. 6, p. 684-690, 2018.

[23] OROZCO, A. C.; FEDERICO, C. A. and GONÇALEZ, O. L. Monte Carlo simulation-assisted project of a thermalization neutron system for neutrongraphy from 241Am-Be sources: Progress report. In: **INTERNATIONAL NUCLEAR ATLANTIC CONFERENCE 2021** (online), virtual meeting, Brazil, November 29 – December 2, 2021.
Available at: < https://inac2021.aben.com.br/resumos/R0589-1.pdf>. Last accessed: 15 May 2022.

[24] ISO - International Organization for Standardization. **Reference neutron radiations – Part 1: Characteristics and methods of production.** ISO 8529-1:2001(E).

[25] MOREIRA, D. S.; KOSKINAS, M. F.; YAMAZAKI, I. M.; DIAS, M. Determination of 51Cr and 241Am X-ray and gamma-ray emission probabilities per decay. **Applied Radiation and Isotopes**, v. 68, n. 4-5, p. 596–599, 2010.

[26] TERADA, K.; NAKAMURA, S.; NAKAO, T.; KIMURA, A.; IWAMOTO, O.; HARADA, H. Measurements of gamma-ray emission probabilities of 241, 243Am and 239Np. **Journal of Nuclear Science and Technology**, v. 53, n. 11, p. 1881-1888, 2016.

[27] LIU, Z.; CHEN, J.; ZHU, P.; LI; Y. The 4.438MeV gamma to neutron ratio for the Am–Be neutron source. **Applied Radiation and Isotopes**, v. 65, n. 12, p. 1318-1321, 2008.

[28] SATO, T.; NIITA, K.; MATSUDA, N.; HASHIMOTO, S.; IWAMOTO, Y.; FURUTA, T.; NODA, S.; OGAWA, T.; IWASE, H.; NAKASHIMA, H.; FUKAHORI, T.; OKUMURA, K.; KAI, T.; CHIBA, S.; SIHVER, L. Overview of particle and heavy ion transport code system PHITS. **Annals of Nuclear Energy**, v. 82, p. 110-115, 2015.

[29] NIITA, K.; IWASE, H.; SATO, T.; IWAMOTO, Y.; MATSUDA, N.; SAKAMOTO, Y.; NAKASHIMA, H.; MANCUSI, D.; SIHVER, L. Recent Developments of the PHITS code. **Progress in Nuclear Science and Technology**, v. 1, p.1-6, 2011.

[30] BLAND, J. M.; ALTMAN, D. G. Measuring agreement in method comparison studies. **Statistical Methods in Medical Research**, v. 8, n. 2, p. 135–60, 1999.

[31] MOHD ALI, N. S.; HAMZAH, K.; JAMRO, R. Simulation of beam collimator for neutron radiography using Monte Carlo method. **Journal of Nuclear and Related Technologies**, v. 13, n. 2, p. 1-12, 2016.

[32] DINCA, M.; PAVELESCU, M; IORGULIS, C. Collimated neutron beam for neutron radiography. **Romanian Journal of Physics**, v. 51, n. 3–4, p. 435–441, 2006.